Sensors and Materials, Vol. 27, No. 2 (2015) 217–227
MYU Tokyo

S & M 1059

SiO_2/SiN Multilayer-Stack Infrared Absorber Integrated on $Pb(Zr_{0.4},Ti_{0.6})O_3$ Film Pyroelectric Sensors on γ-Al_2O_3/Si Substrate

Koji Oishi[1,*], Shota Yonemaru[1], Daisuke Akai[2] and Makoto Ishida[1,2]

[1]Electrical and Electronic Information Engineering, Toyohashi University of Technology, 441-8580 Toyohashi, Aichi, Japan
[2]Electronics-Inspired Interdisciplinary Research Institute, 441-8580 Toyohashi, Aichi, Japan

(Received September 11, 2014; accepted November 25, 2014)

Key words: γ-Al_2O_3, $Pb(Zr,Ti)O_3$, pyroelectric sensor, infrared absorber

In this study, $Pb(Zr_{0.4},Ti_{0.6})O_3$ (PZT) film pyroelectric infrared sensors were fabricated on a Si substrate with a SiO_2/SiN multilayer-stack infrared (IR) absorber and characterized. Since an IR absorber is a critical element that determines the sensitivity of IR sensors, we have proposed a multilayer-stack IR absorber based on complementary metal-oxide-semiconductor (CMOS) compatible materials for the PZT film pyroelectric sensor. We designed and fabricated a SiO_2/SiN multilayer-stack IR absorber that possesses a broad and high IR absorptance in the wavelength range from 8 to 14 μm. The thicknesses of the SiO_2 and SiN films were designed as 550 and 850 nm, respectively, according to the calculation result of absorptance in the multilayer films. The SiO_2/SiN multilayer-stack absorber was integrated on PZT film sensors by plasma-enhanced chemical vapor deposition, and 86% average IR absorptance was obtained in the wavelength range from 8 to 14 μm. A specific detectivity of 1.15×10^7 $cmHz^{0.5}/W$ was achieved at 30 Hz on the PZT film pyroelectric sensor.

1. Introduction

Micro-electromechanical systems (MEMS) on Si substrates have received considerable attention owing to the advantage of circuit integration that enables the miniaturization and functionalization of MEMS device chips. Numerous types of electronic materials and microstructures on Si substrates have been investigated. Among the electronic materials, $Pb(Zr,Ti)O_3$ (PZT) films have been frequently used for MEMS

*Corresponding author: e-mail: oishi-k@int.ee.tut.ac.jp

devices because of their suitable electronic and mechanical properties that enable their application in sensors, actuators, and memories. As one sensor application, human detection using infrared (IR) rays has been desired owing to an increasing demand for applications such as night vision, surveillance, medical monitoring, and environmental monitoring.

Pyroelectric sensors are thermal IR sensors that detect polarization changes in the film when their temperature varies. As in the case of other thermal IR sensors, incident IR radiation needs to be transformed into heat. PZT films are ferroelectric materials commonly used in pyroelectric sensors and have been widely researched because the electronic properties of PZT films can be improved by optimizing many factors such as composition, crystalline orientation, and process conditions. The crystalline PZT films are expected to exhibit superior ferroelectric properties that will improve the performance of pyroelectric sensors as compared with polycrystalline PZT films. We have proposed the integration of crystalline PZT films using γ-Al_2O_3/Si substrates.(1–4) The γ-Al_2O_3 film is used as a buffer layer to realize the PZT film integration for matching the lattice constants of the films. We have successfully fabricated a crystalline PZT film capacitor using $SrRuO_3$, Pt, and γ-Al_2O_3 crystalline films deposited on a Si substrate. A schematic of the sensor structure is shown in Fig. 1. After the integration of the PZT films on the Si substrate, the fabrication of an IR absorber on the pyroelectric sensors would be the next challenge since the PZT films are easily damaged and delaminated during complex processes. Therefore, an IR absorber with a stable structure and requiring a simple fabrication process is desired for application in PZT film pyroelectric sensors.

IR absorption on sensor elements plays a significant role in thermal IR sensors since it strongly influences the sensitivity. Many different absorbers, such as metal-black films,(5) SiN films,(6) and metamaterials,(7) have been investigated. Amongst these absorbers, Au-black films are the most frequently used infrared absorbers because they possess a high IR absorptance of over 90% in wide spectral ranges. Au-black films are extremely porous and of low density, and correspondingly exhibit low heat capacity. However, the highly porous films are difficult to handle since they are fragile, which

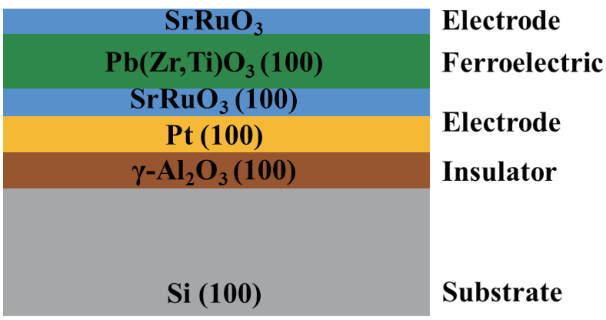

Fig. 1. (Color online) Cross-sectional schematic of PZT film sensor integrated on a γ-Al_2O_3/Si substrate. The $SrRuO_3$ and Pt films were deposited as the top and bottom electrodes, respectively.

makes their patterning a challenge. In sensor fabrication, Au-black films should be coated solely on the sensor structure to realize a temperature difference between the sensor and the substrate, but process limitations of Au-black-film patterning make the fabrication processes complex. Although various patterning processes for Au-black films, such as a lift-off process,(8) stencil lithography,(9) and laser ablation,(10) have been investigated, these processes have disadvantages in terms of alignment accuracy and process speed that are not suitable for integrated device fabrication. The use of Au-black films as IR absorbers complicates the fabrication processes.

In contrast, multilayer-stack IR absorbers have received considerable interest owing to their simple fabrication processes and stable nature during any fabrication processes.(11) The IR absorptance of multilayer-stack absorbers can be improved by optical interferences in multilayer films. Similar methods have been used in thermo-mechanical IR sensors having an optical air cavity with a suitable depth underneath the bimaterial membrane or cantilevers.(12) SiN films are known as IR-absorbing films and frequently used in the thermo-mechanical IR sensors; however, a high IR absorptance cannot be obtained without the optical air cavity underneath sensor structures, and cannot be realized in our proposed crystalline PZT film pyroelectric sensors formed on a γ-Al_2O_3/Si substrate. Therefore, an investigation of multilayer-stack IR absorbers that can be easily deposited on sensor structures is desired.

In this paper, a simply fabricated multilayer-stack IR absorber on a PZT film pyroelectric sensor using CMOS-compatible materials, SiO_2 and SiN, was proposed, designed, fabricated, and characterized. The electrical properties of the PZT film integrated with the multilayer-stack absorber were characterized. Sensor layouts were also designed on the basis of the results of transient heat transfer analysis to improve the IR detectivities of the sensors. The detectivities of the fabricated sensors with different layouts were characterized.

2. Materials and Methods

2.1 *Design of SiO_2/SiN multilayer-stack IR absorber*

The materials proposed for the multilayer-stack IR absorber are SiO_2 and SiN films deposited by plasma-enhanced chemical vapor deposition (PECVD). The advantages of SiO_2 and SiN films as IR absorbers are as follows: not only are they CMOS-compatible materials with IR absorption peaks, but also they act as interlayer dielectrics for the top and bottom electrodes of the PZT film. Owing to their stable structures, they are easily integrated and patterned via conventional photolithography processes. The IR absorption peaks of SiO_2 and SiN films are at wavelengths of approximately 10 and 12 μm, respectively. In order to obtain a broad spectral range of IR absorption from 8 to 14 μm that is commonly applied for human detection, we have stacked SiO_2 and SiN films to form a SiO_2/SiN structure.

The multilayer-stack absorber was designed to absorb IR radiation efficiently. Suitable thicknesses of SiO_2 and SiN films were estimated by optical calculations. A SiO_2/SiN/Pt/Si structure was considered for calculating IR absorption in the wavelength range from 8 to 14 μm. The IR absorptance was calculated from the reflectance of the multilayer films. The reflectance calculation model is shown in Fig. 2. We assumed the incident IR radiation to be perpendicular to the sample surface. Since the Pt film was deposited underneath the SiO_2/SiN films, the IR radiation was expected to not be transmitted through the Pt film owing to the large difference in their refractive index. Therefore, the absorptance was calculated from the IR radiation that was not reflected from the multilayer structure. The reflectance calculations were started by deriving the reflectance coefficient from the bottom interface to the top interface, and the square of the overall reflectance coefficient was calculated to obtain the total reflectance. The reflectance coefficients were calculated using the following equations:

$$R = |r_m|^2 = \left| \frac{r_{m+1,m} + r_{m-1} e^{i\Delta m}}{1 + r_{m-1} r_{m+1,m} e^{i\Delta m}} \right|^2 \quad (m > 0), \tag{1}$$

$$r_{i,j} = \frac{n_i^* \cos\theta_i - n_j^* \cos\theta_j}{n_i^* \cos\theta_i + n_j^* \cos\theta_j}, \tag{2}$$

$$r_0 = r_{1,0}, \tag{3}$$

$$\Delta_m = \frac{4\pi n_m^* d\cos\theta_m}{\lambda}, \tag{4}$$

where R and r are the total reflectance and reflectance coefficient respectively. The integer subscript m denotes the number of films, which is 3 in this case. θ is the incidence and refraction angle of the IR ray. n^* is the complex index of refraction. d is the layer thickness. λ is the wavelength of the IR ray. We have defined n_4^*, n_3^*, n_2^*, n_1^*, and n_0^* as complex indexes of air, SiO_2, SiN, Pt, and Si, respectively.

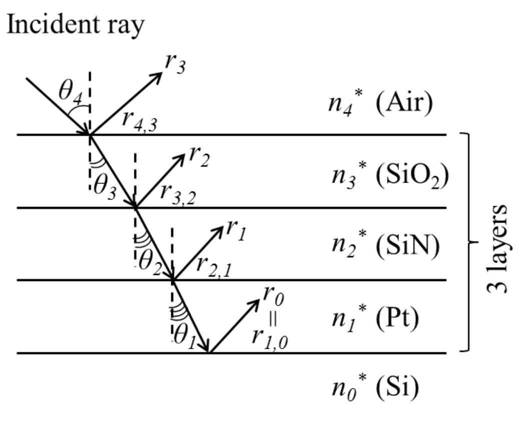

Fig. 2. Reflectance calculation model of multilayer films consisting of a SiO_2/SiN/pt/Si structure.

From the above calculation, the maximum absorption efficiency was obtained with the SiO_2(550 nm)/SiN(850 nm) multilayer-stack structure. The complex refractive indexes of the SiO_2 and SiN films used in the calculation were obtained from refs. 13 and 14. The thickness of the Pt film was 70 nm. The SiO_2/SiN structure was fabricated by PECVD on a Pt/Si substrate. The Pt film was deposited on the Si substrate by a sputtering process. Absorptance was measured by Fourier transform infrared spectroscopy (FTIR). Because the Pt film has a high IR reflectance of around 98%, the absorptance of the SiO_2/SiN film on a Pt/Si substrate can be calculated by measuring the total reflectance of the sample. The IR rays were irradiated perpendicularly to the film surface. The calculated and measured absorption characteristics of the SiO_2/SiN multilayer-stack structure on the Pt/Si substrate are shown in Fig. 3. An average absorptance of 70% was achieved with the SiO_2(550 nm)/SiN(850 nm) multilayer-stack structure in the wavelength range from 8 to 14 µm, and well matched the calculated result. An IR absorber based on a SiO_2/SiN multilayer-stack structure with a broad spectral range was successfully designed and fabricated.

2.2 *Design of sensor layout*

Layouts of pyroelectric sensors were designed on the basis of the results of the simulations of transient heat transfer analyses using a finite element model. Sensors with beam lengths of 200 and 1000 µm were designed as shown in Fig. 4, and transient heat transfer analyses of those sensor structures were simulated. The beam width was 10 µm. In the simulations, a heat flux of 100 W/m^2, which is expected to be emitted from the human body, was input on the surface of the IR absorber. Square waves of the heat flux were set as input to represent the chopped incident IR rays used in an actual IR detection in pyroelectric sensors. Simulation results for two sensors with different beam lengths are shown in Fig. 5. Sensors with different maximum temperatures were obtained. These sensors were fabricated for characterization.

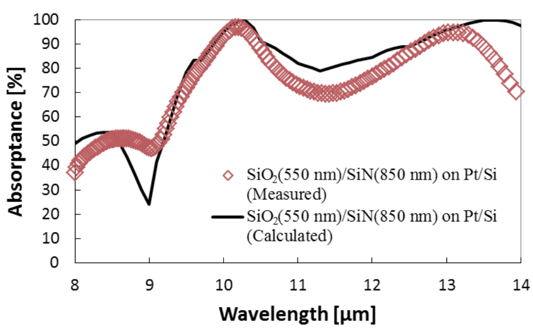

Fig. 3. (Color online) Calculated and measured absorptance characteristics of a SiO_2(550 nm)/SiN(850 nm) multilayer-stack IR absorber on a Pt(70 nm)/Si substrate .

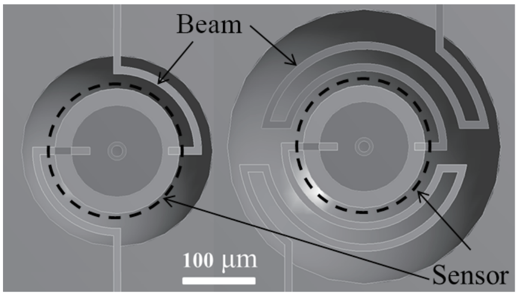

Fig. 4. Layouts of sensor structures with beam lengths of 200 (left) and 1000 μm (right). The beams width is 10 μm. The area of the IR detector is 11775 μm².

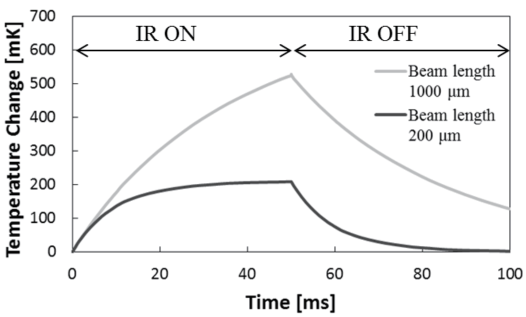

Fig. 5. Transient heat transfer analysis results of designed sensor structures with beam lengths of 200 and 1000 μm.

2.3 *Fabrication*

The fabrication processes of the crystalline PZT film pyroelectric sensor with the SiO_2/SiN multilayer-stack IR absorber on a Si substrate are illustrated in Fig. 6. First, a crystalline γ-Al_2O_3 film of 50 nm thickness was grown on a Si substrate at 960 °C using trimethylaluminum and O_2 gases by metal organic chemical vapor deposition as shown in Fig. 6(a). Then, Pt and $SrRuO_3$ films of 70 and 10 nm thicknesses were deposited at 600 and 750 °C, respectively, by sputtering for the bottom electrode of the pyroelectric sensor. The sol-gel method was used to deposit a 450-nm-thick PZT film. The composition of Zr to Ti ratio was 40/60, which is preferable for pyroelectric sensors. Then, the film was crystallized at 650 °C for 90 s by rapid thermal annealing (RTA) in O_2 atmosphere. The top electrode of a 100-nm-thick $SrRuO_3$ film was deposited by sputtering at room temperature. The sensors were then patterned by inductively coupled plasma reactive ion etching as shown in Fig. 6(c). A SiO_2/SiN multilayer-stack IR absorber was then deposited by PECVD. An Al film was sputtered for the metallization process shown in Fig. 6(e). Finally, the fabricated sensor was thermally isolated by Si etching using XeF_2 gases.

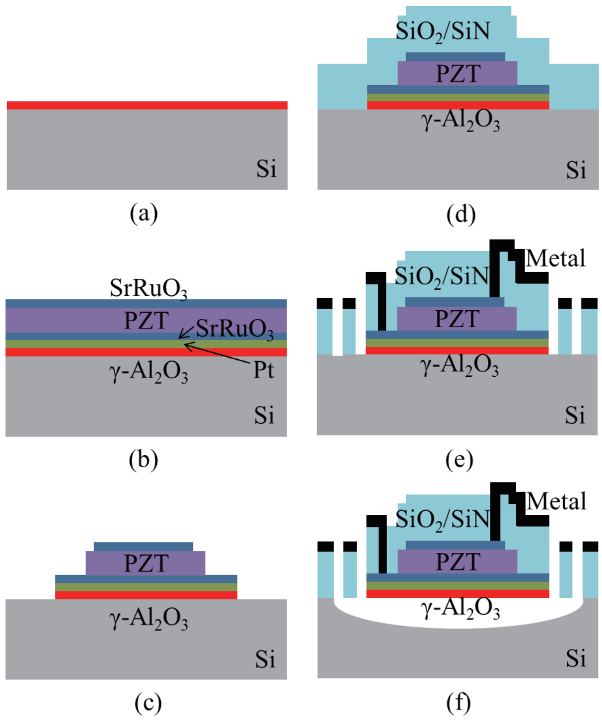

Fig. 6. (Color online) Fabrication processes for a PZT film pyroelectric sensor integrated with a SiO_2/SiN multilayer-stack absorber. (a) Growth of crystalline a γ-Al_2O_3 film on a Si substrate, (b) deposition of Pt, $SrRuO_3$, and PZT films, (c) patterning of a sensor structure, (d) deposition of a SiO_2/SiN multilayer-stack structure, (e) patterning of a SiO_2/SiN multilayer-stack structure and metallization, and (f) Si etching underneath sensor structure.

3. Results and Discussion

Figure 7 shows a scanning electron microscopy (SEM) image of a fabricated PZT pyroelectric sensor with the SiO_2/SiN multilayer-stack IR absorber. Sensors with beam lengths of 200 and 1000 μm were both successfully fabricated. The beams appear to be twisted owing to the high stresses that the Al and SiO_2/SiN films underwent after the release of the sensor structure from the Si substrate. Although the beams were twisted, the sensor surface remained parallel to the substrate; therefore, this sensor was still considered to receive incident IR rays efficiently. In order to reduce film stress, the modification of Al and SiO_2/SiN deposition conditions was required. Polarization hysteresis loops of sensors with beam lengths of 200 and 1000 μm are characterized in Fig. 8. Spontaneous polarizations of 28 and 33 μC/cm^2 were obtained in sensors with beam lengths of 200 and 1000 μm, respectively. The spontaneous polarization values were relatively high for the PZT film compared with other reports such as refs. 15 and 16, and superior performance for IR detection was expected.

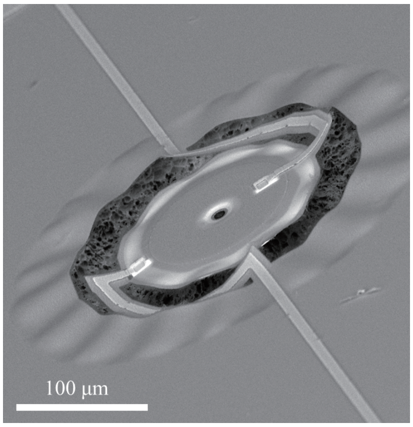

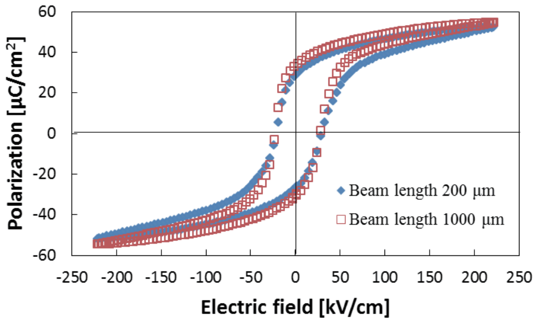

Fig. 7 (left). SEM image of the fabricated PZT film pyroelectric sensor with a SiO_2/SiN multilayer-stack IR absorber. The beam length is 200 μm.
Fig. 8 (right). (Color online) Absorption characteristics of the SiO_2/SiN deposited PZT film pyroelectric sensor on a γ-Al_2O_3/Si substrate and the SiO_2/SiN deposited on a Pt/Si substrate measured by FTIR.

Absorption characteristics of the SiO_2/SiN deposited PZT film pyroelectric sensor were measured by FTIR as shown in Fig. 9. Although the $SrRuO_3$/PZT/$SrRuO_3$ sensor structure is transparent to IR rays, it still absorbs a small amount of IR rays. The IR absorptance of the SiO_2/SiN/$SrRuO_3$/PZT/$SrRuO_3$/Pt/γ-Al_2O_3/Si structure was considered to be improved. As a result, a further improved and broader IR absorptance range was obtained. An average absorptance of 86% in the wavelength range from 8 to 14 μm was achieved with the fabricated multilayer-stack IR absorber integrated PZT film pyroelectric sensor.

An important sensor parameter that describes the performance of IR detection is specific detectivity (D^*) derived by the following equations:

$$D^* = \frac{\sqrt{A_S}}{V_N} R_V, \tag{5}$$

$$R_V = \frac{V_S}{\Phi_S}, \tag{6}$$

where A_S is the area of the IR sensor, V_N is the noise voltage, and R_V is the responsivity derived from the division of the signal voltage V_S from the radiant flux Φ_S. The unit of D^* is cmHz$^{0.5}$/W.[17] Since the output signal voltage of the pyroelectric sensor is measured using a lock-in amplifier, root mean square values of the detected signal voltages were used for determining the signal voltage V_S.

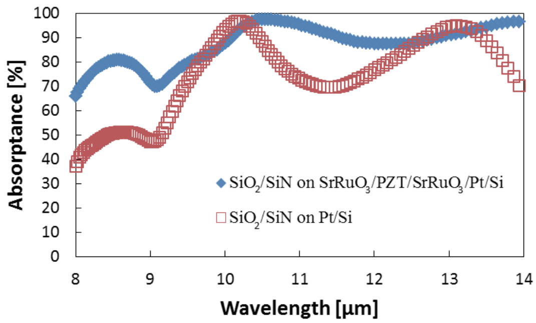

Fig. 9. (Color online) Polarization hysteresis loops of the fabricated PZT film pyroelectric sensors with a SiO_2/SiN multilayer-stack IR absorber.

The block diagram of the detectivity measurement system is shown in Fig. 10. The fabricated PZT film pyroelectric sensors were packaged with a discrete junction field effect transistor (2SK3796) and a resistor (470 kΩ) to obtain a source-follower circuit. They have been packaged in a TO-5 package and covered by a metal cap with an IR filter window. The IR filter used in the measurement was a long-pass filter with 70% average IR transmission in the wavelength range from 6 to 13 µm. A blackbody emitter was placed 20 cm from the sensor package, and a mechanical chopper was placed in front of the blackbody emitter. The output of the source-follower circuit was connected to a lock-in amplifier, which was also synchronized with the chopper frequency. D^* values of the packaged sensor with beam lengths of 200 and 1000 µm were measured up to a frequency of 45 Hz as shown in Fig. 11. As a result, D^* of 1.15×10^7 cmHz$^{0.5}$/W at 30 Hz chopping frequency was obtained in the fabricated PZT film pyroelectric sensor with the SiO_2/SiN multilayer-stack IR absorber for a beam length of 1000 µm. In the pyroelectric sensor, the output signal could be obtained only when the temperature of the PZT film changed. Therefore, D^* improved as the chopping frequency increased. In contrast, D^* decreased at a low chopping frequency, because the temperature of the PZT film saturated. Therefore, the temperature of the PZT sensor must not saturate during the IR chopping cycles, which are the repeat of IR-irradiated and nonirradiated states. D^* became maximum in the 20-to-40 Hz chopping frequency range, and appeared to start decreasing at chopping frequencies higher than 40 Hz. The absolute temperature change in the sensor structure is also considered to be important at a high chopping frequency. The relationship between the measured D^* values and the transient heat transfer analysis simulation results shown in Fig. 5 was investigated. The D^* of the sensor with a beam length of 1000 µm at 10 Hz was about 1.3 times higher than that of the sensor with a beam length of 200 µm, while the root mean square value of the time derivative of the simulated temperature change in the sensor with a beam length of 1000 µm was calculated as being 1.78 times higher than that for the sensor with a beam length of 200 µm. The transient heat transfer analysis simulation results matched with the improved D^* in the actual sensor structure. Therefore, the transient heat transfer analysis simulation can be used to estimate the D^* of the designed sensor.

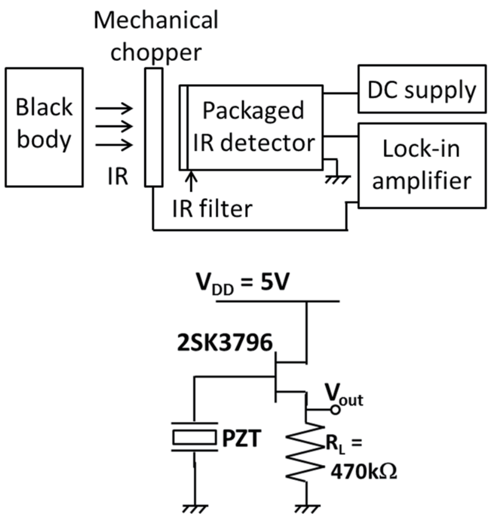

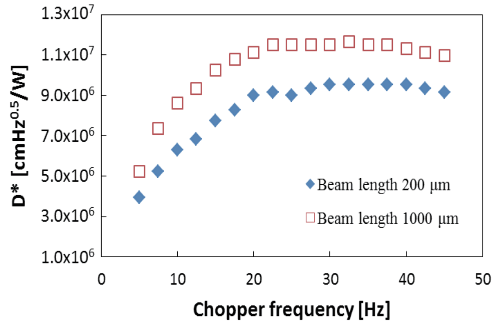

Fig. 10 (left). Measurement system of IR detection consists of a blackbody emitter, a mechanical chopper, an IR detector, a 5 V DC supply, and a lock-inamplifier. The sensor was packaged with a discrete junction field effect transistor and a resistor.
Fig. 11 (right). (Color online) Detectivity of the fabricated PZT film pyroelectric sensors with SiO_2/SiN multilayer-stack absorber.

4. Conclusion

A simply fabricated multilayer-stack IR absorber consisting of SiO_2/SiN was successfully designed and applied in a PZT film pyroelectric sensor formed on a γ-Al_2O_3/Si substrate. A high IR absorptance in a broad spectral range was obtained with a SiO_2(550 nm)/SiN(850 nm) film. An average IR absorptance of 86% was achieved in the multilayer-stack IR absorber deposited PZT film pyroelectric sensor in the wavelength range from 8 to 14 μm. The sensor layout was also designed on the basis of the results of transient heat transfer analysis simulation. As a result, D^* of 1.15 × 107 cmHz$^{0.5}$/W was obtained at a 30 Hz chopping frequency. The multilayer-stack absorber using CMOS-compatible materials is a suitable IR absorber for PZT film pyroelectric sensors.

References

1 D. Akai, K. Sawada and M. Ishida: J. Cryst. Growth **259** (2003) 90.
2 D. Akai, K. Hirabayashi, M. Yokawa, K. Sawada and M. Ishida: J. Cryst. Growth **264** (2004) 463.
3 D. Akai, K. Hirabayashi, M. Yokawa, K. Sawada, Y. Taniguchi, S. Murashige, S. Murashige, N. Nakayama, T. Yamada, K. Murakami and M. Ishida: Sens. Actuators, A **130–131** (2006) 111.
4 Y. Guo, D. Akai, K. Sawada and M. Ishida: Solid State Commun. **145** (2007) 413.

5 R. R. Neli, I. Doi, J. A. Diniz and J. W. Swart: Sens. Actuators, A **132** (2006) 400.
6 Y. Zhao, M. Mao, R. Horowitz, A Majumdar, J. Varesi, P. Norton and J. Kitching: J. Microelectromech. Syst. **11** (2002) 136.
7 N. Zhang, P. Zhou, S. Zou, X. Weng, J. Xie and L. Deng: Prog. Nat. Sci. **24** (2014) 128.
8 M. Hirota, Y. Nakajima, M. Saito and M. Uchiyama: Sens. Actuators, A **135** (2007) 146.
9 D. Panjwani, M. Yesiltas, S. Singh, E. D. Barco, R. E. Peale, C. Hirschmugl and J. Sedlemair: Infrared Phys. Technol. **66** (2014) 1.
10 N. Nelms, J. Dowson, N. Rizvi and T. Rohr: Appl. Opt. **45** (2006) 6977.
11 M. Laamanen, M. Blomberg, R. L. Puurunen, A. Miranto and H. Kattelus: Sens. Actuators, A **162** (2010) 210.
12 M. F. Toy, O. Ferhanoglu, H. Torun and H. Urey: Sens. Actuators, A **156** (2009) 88.
13 A. Andersen, H. Mutschke, T. Posch, M. Min and A Tamanai: J. Quant. Spectrosc. Radiat. 100 (2006) 4.
14 F. Jutzi, D. Wicaksono, G. Pandraud, N. Rooij and P. French: Sens. Actuators, A **152** (2009) 119.
15 C. Zinck, D. Pinceau, E. Defay, E. Delevoye and D. Barbier: Sens. Actuators, A **115** (2004) 483.
16 M. Kang, K. Kim and C. Kim: Thin Solid Films **398–399** (2001) 448.
17 H. Budzier and G. Gerlach: *Thermal Infrared Sensors Theory, Optimization and Practice*, ed. D. Muller (A John Wiley and Sons, Chichester, 2011) p. 155.